Human Molecular Genetics, 2011, Vol. 20, No. 24 ***4759–4774***
doi:10.1093/hmg/ddr403
Advance Access published on September 8, 2011

Dysregulation of Semaphorin7A/β1-integrin signaling leads to defective GnRH-1 cell migration, abnormal gonadal development and altered fertility

Andrea Messina[1,4], Nicoletta Ferraris[1], Susan Wray[2], Gabriella Cagnoni[1], Duncan E. Donohue[2], Filippo Casoni[2,4], Phillip R. Kramer[2], Alwin A. Derijck[3], Youri Adolfs[3], Aldo Fasolo[1], Ronald J. Pasterkamp[3] and Paolo Giacobini[1,2,4,*]

[1]Department of Human and Animal Biology, University of Turin, Turin 10123, Italy, [2]Cellular and Developmental Neurobiology Section, NINDS, NIH, Bethesda, Maryland 20892, USA, [3]Department of Neuroscience and Pharmacology, Rudolf Magnus Institute of Neuroscience, University Medical Center Utrecht, CG Utrecht 3584, The Netherlands and [4]Inserm, Jean-Pierre Aubert Research Center, Unité 837, Development and Plasticity of the Postnatal Brain, Place de Verdun, Lille Cedex 59045, France

Received July 18, 2011; Revised and Accepted September 2, 2011

Reproduction in mammals is dependent on the function of specific neurons that secrete gonadotropin-releasing hormone-1 (GnRH-1). These neurons originate prenatally in the nasal placode and migrate into the forebrain along the olfactory–vomeronasal nerves. Alterations in this migratory process lead to defective GnRH-1 secretion, resulting in heterogeneous genetic disorders such as idiopathic hypogonadotropic hypogonadism (IHH), and other reproductive diseases characterized by the reduction or failure of sexual competence. Combining mouse genetics with *in vitro* models, we demonstrate that Semaphorin 7A (Sema7A) is essential for the development of the GnRH-1 neuronal system. Loss of Sema7A signaling alters the migration of GnRH-1 neurons, resulting in significantly reduced numbers of these neurons in the adult brain as well as in reduced gonadal size and subfertility. We also show that GnRH-1 cells differentially express the Sema7 receptors β1-integrin and Plexin C1 as a function of their migratory stage, whereas the ligand is robustly expressed along developing olfactory/vomeronasal fibers. Disruption of Sema7A function *in vitro* inhibits β1-integrin-mediated migration. Analysis of *Plexin C1*$^{-/-}$ mice did not reveal any difference in the migratory process of GnRH-1 neurons, indicating that Sema7A mainly signals through β1-integrin to regulate GnRH-1 cell motility. In conclusion, we have identified *Sema7A* as a gene implicated in the normal development of the GnRH-1 system in mice and as a genetic marker for the elucidation of some forms of GnRH-1 deficiency in humans.

INTRODUCTION

Reproduction in vertebrates depends on the secretion of the decapeptide gonadotropin-releasing hormone-1 (GnRH-1) by a small group of neuroendocrine cells located in the preoptic area and/or hypothalamus (1). The synchronized pulsatile release of GnRH-1 from this neural network governs the synthesis and secretion of the anterior pituitary gonadotropin-luteinizing hormone and follicle-stimulating hormone, which in turn stimulate gonadal steroidogenesis and gametogenesis (1). GnRH-1-secreting neurons originate in the nasal placode during embryonic development and migrate to the hypothalamus along olfactory/vomeronasal fibers (2,3). Although the migration of these neurons from the nose to the brain has been documented in a variety of vertebrate species and is thought to be fundamental to the initiation of reproduction, the genetic program underlying the development of the GnRH-1 system is still poorly understood (4). Alterations in this migratory process lead to defects in GnRH-1 secretion and hypogonadotropic hypogonadism in humans, a condition characterized by a reduction or

*To whom correspondence should be addressed. Tel: +33 320622060; Fax: +33 320538562; Email: paolo.giacobini@inserm.fr

failure of sexual competence (5). Idiopathic hypogonadotropic hypogonadism (IHH) is a genetic disease that can occur in association with anosmia (Kallmann syndrome; KS) or with a normal sense of smell (normosmic IHH). To date, mutations in genes involved in the onset of IHH only account for only ~40% of cases, implying that other candidate genes crucial for GnRH-1 neuronal development remain to be discovered (4,5). Moreover, mutations in genes involved in IHH have also recently been found to confer susceptibility to the functional deficiency of GnRH-1 secretion that characterizes other human reproductive disorders, such as hypothalamic amenorrhea (6).

The complex developmental events leading to correct GnRH-1 neuronal migration and secretion are tightly regulated by the specific spatiotemporal expression patterns of growth factors, adhesion molecules, diffusible attractants and repellents (1,7). Recently, various semaphorins have been shown to play a significant role in the control of this migratory process (8–10). The semaphorins constitute one of the largest families of phylogenetically conserved proteins, serving as guidance cues (11). Although originally identified as embryonic axon guidance cues, semaphorins are now known to regulate multiple processes crucial for neuronal network formation (12). The experiments presented in this paper focus on Semaphorin 7A (Sema7A), the only glycosyl-phosphatidylinositol-anchored protein in the semaphorin family (13–15). The function of Sema7A has been studied most extensively in the context of immune cell function (16) and cancer cell biology (17–19), with few reports addressing its neuronal role (20–22). Sema7A can act either as a membrane-bound signaling molecule or as a soluble factor following proteolytic cleavage (12). It binds to Plexin C1 to decrease integrin-mediated cell attachment and spreading (18) and to β1-integrin to induce integrin clustering and the activation of MAPK pathways (22). The prominent expression of Sema7A in different areas of the brain suggests a role for this molecule in neuronal migration and/or axonal elongation (23,24). The Sema7A transcript has been documented in the main and accessory olfactory systems, including the vomeronasal organ where GnRH-1 neurons originate, and its receptor, Plexin C1, has also been localized to GnRH-1 neurons (24). This expression pattern prompted us to investigate the potential role of Sema7A in GnRH-1 neuronal migration.

Using different genetic mouse models as well as *in vitro* manipulation, we provide direct evidence for a role for Sema7A signaling in the establishment of the GnRH-1 system. The loss of Sema7A/β1-integrin signaling leads to defective GnRH-1 cell migration, an aberrant GnRH-1 system and altered fertility. These results raise the possibility that genetic defects in components of the Sema7A pathway could lead to deficient GnRH-1 signaling and reproductive dysfunctions in humans.

RESULTS

Sema7A is expressed in the developing olfactory system

To determine the role of Sema7A in the developing GnRH-1 and olfactory systems, we examined the spatiotemporal expression pattern of Sema7A during mouse embryonic development using *in situ* hybridization and immunohistochemistry. At E11.5, when GnRH-1 neurons were beginning to migrate out of the presumptive vomeronasal organ (vno; Fig. 1A), Sema7A mRNA was detectable in the vomeronasal organ and olfactory epithelium (oe; Fig. 1B). A similar expression pattern was detected at E12.5 and E14.5 (data not shown). Double-immunofluorescence labeling for GnRH-1 (red) and Sema7A (green) at E12.5 and E14.5 (data not shown) confirmed Sema7A expression in the developing olfactory sensory neurons as well as along their axons projecting to the forebrain (Fig. 1C and D), In contrast, Sema7A was not found in migrating GnRH-1 neurons (Fig. 1D, inset). Olfactory–vomeronasal axons express neural cell adhesion molecule (NCAM) (25,26) and peripherin, whereas GnRH-1 cells in the mouse do not (27,28). In order to confirm that the Sema7A-immunopositive fibers in our samples were olfactory axons, we performed double-immunofluorescence labeling for Sema7A and NCAM (Fig. 2A–I). The expression patterns for the two markers overlapped in fibers emerging from the vomeronasal organ at E12.5 (Fig. 2D–F) and in olfactory/vomeronasal axon bundles entering the forebrain (Fig. 2G–I).

Since olfactory ensheathing cells, which accompany and ensheath the primary olfactory axons, have been previously shown to bear some NCAM immunoreactivity (26), we cannot exclude that these cells could represent an additional source of Sema7A.

These results demonstrate that, during early embryonic development, Sema7A demarcates the pathway along which GnRH-1 neurons migrate.

Primary GnRH-1 neurons differentially express β1-integrin and Plexin C1 as a function of migratory stage

The expression pattern of Sema7A along the olfactory/vomeronasal axonal scaffold suggested that this molecule could play a role in the migratory process of GnRH-1 neurons. To determine whether GnRH-1 neurons could respond to Sema7A signaling, we investigated the expression of Sema7A receptors in migratory and post-migratory GnRH-1 neurons from nasal explants. Nasal explants permit spatial and temporal cues to be distinguished, and the properties of GnRH-1 neurons to be identified, by controlling extracellular influences (29,30). Single-cell cDNA sets from migratory (4 days *in vitro*, DIV) and post-migratory (10 DIV) GnRH-1 cells were generated (31,32) and subsequently screened on GeneChip microarrays to examine the relative expression of known genes encoding various molecules linked to the Sema7A signaling pathway. GnRH-1 neurons expressed β1-integrin (Itgb1) at comparable levels in the migratory and post-migratory stages, whereas the expression of the other Sema7A receptor, Plexin C1 (Plxnc1), was absent in migratory cells and expressed in post-migratory GnRH-1 neurons (Supplementary Material, Fig. S1A and B). The expression profiles determined by microarray screening were verified by single-cell RT-PCR performed on GnRH-1 neurons (data not shown). These findings indicate that during the migratory phase Sema7A acts on GnRH-1 cells through β1-integrin.

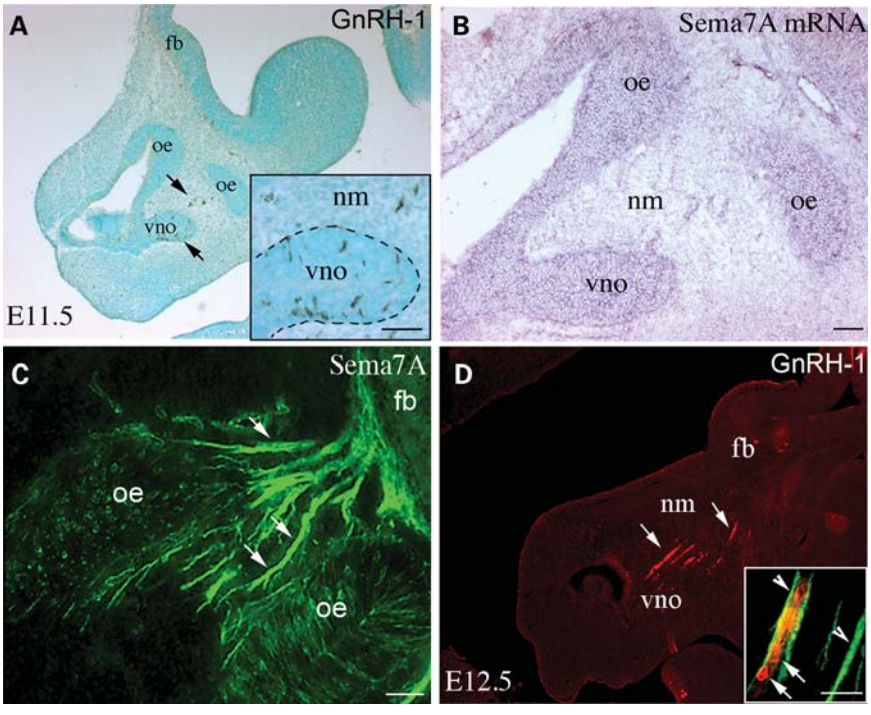

Figure 1. Sema7A is expressed in the developing olfactory/vomeronasal systems and in the olfactory bulb. (**A**) Immunohistochemistry for GnRH-1 on a sagittal section of an E11.5 embryo. GnRH-1-immunoreactive cells are located within the developing vomeronasal organ (vno) and in the nasal mesenchyme (nm), where they can be seen migrating directed toward the forebrain (fb). Immunoreactive cells are indicated by black arrows. (**B**) *In situ* hybridization for Sema7A on an adjacent sagittal section from the same animal. Sema7A mRNA is distributed in the developing olfactory epithelium (oe) as well as in the vno. (**C**) Immunohistochemistry for Sema7A on a sagittal section of an E12.5 embryo showing immunoreactivity in the developing olfactory sensory neurons and along their axons (arrows). (**D**) Sagittal section of an E12.5 mouse nose double-labeled for GnRH-1 (red; C) and Sema7A (green) shows the complementary expression patterns of the two antigens. Sema7A is expressed by the olfactory/vomeronasal axons along which GnRH-1-immunoreactive cells migrate (see inset in D). Scale bars: (A) 130 μm, inset in (A) 40 μm, (B) 60 μm, (C) 50 μm, (D) 200 μm and inset in (D) 20 μm.

Expression of Sema7A receptors in the developing nasal region

To confirm the microarray data, the spatiotemporal expression pattern of Plexin C1 and β1-integrin proteins was investigated in sections of E12.5–15.5 mouse heads. Immunofluorescent labeling for GnRH-1 (Fig. 3A–C) and β1-integrin (Fig. 3D and E) was carried out using consecutive sagittal sections at E12.5. The antibody to β1-integrin labeled a large group of cells migrating out of the vomeronasal organ in chain-like structures and crossing the nasal mesenchyme (Fig. 3D and E, see arrows in D). Notably, these cells had the same distribution as the GnRH-1 migratory neurons detected in adjacent sections (Fig. 3A–C, see arrows in A), suggesting the expression of β1-integrin by GnRH-1 cells during the initial stages of their migratory process.

It has previously been reported that the Plexin C1 transcript is present in the vomeronasal organ and olfactory epithelium as well as in some GnRH-1 migratory cells in the nasal compartment during embryonic development in the rat (24). Double-immunofluorescence labeling was performed at E12.5 for Plexin C1 and peripherin, a marker of the olfactory/vomeronasal system (28). At this stage, Plexin C1 was expressed exclusively along olfactory/vomeronasal axons (Fig. 3G and H), and was not detectable in cell bodies located in the nasal mesenchyme. In order to confirm the absence of Plexin C1 expression by GnRH-1 neurons in nasal regions, sections adjacent to those labeled for Plexin C1 and peripherin (Fig. 3J) were immunolabeled for GnRH-1 (Fig. 3I), and the resulting images were superimposed. Plexin C1 expression was seen to be confined to olfactory/vomeronasal axons (see arrow, Fig. 3J), whereas Plexin C1-negative GnRH-1-immunoreactive cells were apposed to this axonal scaffold (see arrowheads).

The Plexin C1 transcript has been found in GnRH-1 cells in the rat at E16–E19 (24). This suggests that the expression of Plexin C1 may vary as a function of age, consistent with the results of the microarray analysis.

Immunofluorescence analysis at E15.5 in the mouse revealed that GnRH-1 and Plexin C1 were co-expressed in GnRH-1 neurons within the basal forebrain (Fig. 3K–M). Overall, these data indicate that β1-integrin, Plexin C1 and Sema7A interact differentially in GnRH-1 neurons as a function of age and location.

Altered migration of GnRH-1 neurons in *Sema7A*$^{-/-}$ mice leads to suboptimal GnRH-1 cell numbers in the adult brain and to impaired fertility

The phenotype of *Sema7A*$^{-/-}$ mice was analyzed to determine whether the lack of this molecule impacted the development of the GnRH-1 system. The number of GnRH-1 cells in the nasal compartment, olfactory bulb/dorsal forebrain area

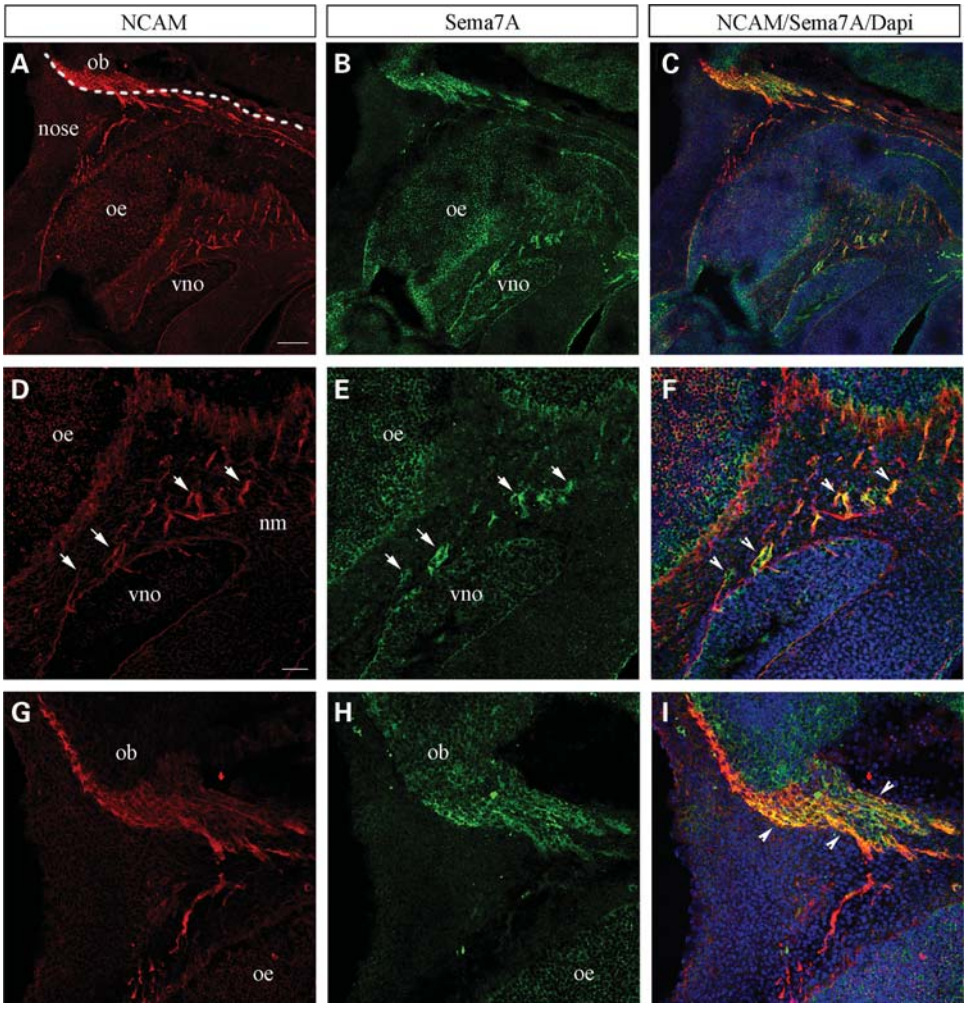

Figure 2. Expression of Sema7A on olfactory and vomeronasal axons. (**A**–**I**) Sagittal sections of E14.5 mouse heads show that Sema7A is localized in NCAM-positive olfactory/vomeronasal axons in the nasal compartment. Dashed line in (A) represents the boundary between the nasal compartment and the forebrain. Arrows in (D) and (E) indicate, respectively, NCAM- and Sema7A-immunoreactive vomeronasal axons; arrowheads in (F) show co-localization of the two antigens along these fibers. (G–I) High-magnification pictures of the bundle of olfactory/vomeronasal axons contacting the developing olfactory bulb. Arrowheads in (I) indicate Sema7A/NCAM co-expression along these fibers. vno, vomeronasal organ; oe, olfactory epithelium; nm, nasal mesenchyme; ob, olfactory bulb. Scale bars: (A–C) 100 μm, (D–I) 50 μm.

(ob/dfb) and ventral forebrain (vfb) of E14.5 embryos was determined (Fig. 4E). In mutants, GnRH-1 neurons accumulated in the nasal compartment (Fig. 4A and B versus C and D), resulting in approximately twice as many GnRH-1 cells as in wild-type (WT) mice (Fig. 4F). Concomitantly, fewer GnRH-1 cells reached the brain in *Sema7A*$^{-/-}$ embryos compared with WT littermates (Fig. 4F). The fact that the total number of GnRH-1-positive cells was unchanged in *Sema7A*$^{-/-}$ embryos indicates the absence of a defect in the proliferation/survival of these cells in mutant mice. Thus, the change in the distribution of GnRH-1 cells in *Sema7A*$^{-/-}$ mice is consistent with a migratory deficit. In order to determine whether this change was due to defective navigation by olfactory axons, the expression pattern of peripherin was compared in WT and *Sema7A*$^{-/-}$ embryos (Supplementary Material, Fig. S2A–F). The loss of Sema7A did not overtly alter the innervation of the developing olfactory bulb by olfactory/vomeronasal axons (Supplementary Material, Fig. S2A–E). The caudal branch of the vomeronasal nerve, which guides GnRH-1 neuronal migration into the hypothalamic target area, was also similar in WT and mutant mice (Supplementary Material, Fig. S2C and F). These results demonstrate that the alteration in GnRH-1 neuronal migration observed in *Sema7A*$^{-/-}$ mice is not caused by developmental defects in the olfactory system.

To determine whether the delay in GnRH-1 cell migration affects the size of this neuronal population in adult brains, the number and distribution of GnRH-1 cells was analyzed in WT and mutant mice. A 30% reduction in the total number of GnRH-1 neurons was detected in *Sema7A*$^{-/-}$ adult mice (Fig. 4G). Moreover, whereas many GnRH-1-immunoreactive fibers innervated the median eminence (me) in WT animals, GnRH-1 innervation was clearly reduced in *Sema7A*$^{-/-}$ animals (Fig. 4H and I).

The observation that transgenic mice possess fewer GnRH-1 neurons suggests that fertility might be disrupted. To

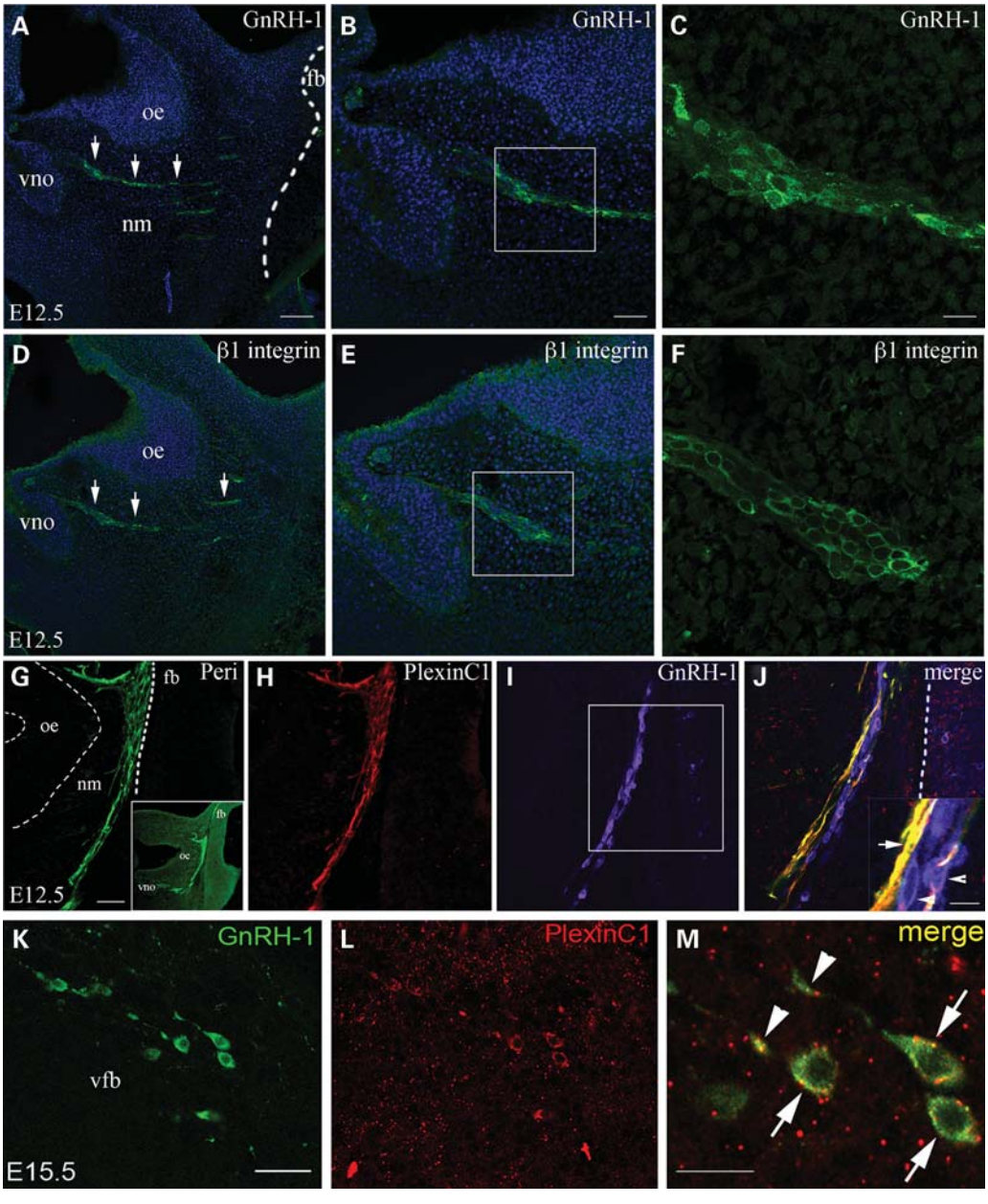

Figure 3. Differential expression of Sema7A receptors in GnRH-1 neurons *in vivo*. (**A**–**C**) Sagittal section of an E12.5 embryo labeled for GnRH-1. Arrows indicate chains of GnRH-1 neurons migrating out of the vomeronasal organ (vno) and crossing the nasal mesenchyme. Dashed lines indicate the border between the nose and the forebrain. High magnification of the box in (B) is shown in (C). (**D**–**F**) β1-Integrin immunoreactivity on an adjacent sagittal section from the same animal, resembling the labeling pattern for GnRH-1 (arrows in D). (**G** and **H**) Double-immunofluorescence labeling for peripherin (G) and Plexin C1 (H) indicates the co-expression of these antigens along olfactory/vomeronasal axons crossing the nasal mesenchyma (nm). Inset in (G) shows a low-magnification image of the E12.5 sagittal section immunolabeled for peripherin. (**I**) An adjacent section immunolabeled for GnRH-1. (**J**) Superimposition of (G), (H) and (I) shows that GnRH-1 neurons migrate along peripherin/Plexin C1-positive axons (arrow in the inset) but do not themselves express either peripherin or Plexin C1 (arrowheads in the inset). (**K**–**M**) Double-immunofluorescence labeling performed on sagittal sections of an E15.5 mouse embryo for GnRH-1 and Plexin C1. Co-expression of the two antigens is detectable in GnRH-1 neurons located in the ventral forebrain. Arrows in (M) indicate Plexin C1 expression in GnRH-1 cell bodies, whereas arrowheads highlight Plexin C1-immunoreactivity along GnRH-1 neurites. Scale bars: (A and D) 40 μm, (B and E) 20 μm, (C and F) 10 μm, (G–J) 20 μm, inset in (G) 100 μm, inset in (J) 10 μm, (K–M) 20 μm, inset in (M) 10 μm.

determine this, WT, *Sema7A*$^{+/-}$ and *Sema7A*$^{-/-}$ mice were crossed, and the resulting litter sizes were examined. A significant reduction in the number of pups per litter was seen when *Sema7A*$^{-/-}$ mice were bred (Fig. 4J). In order to investigate the possible existence of a gonadal defect in males, the morphology of the testes of WT and knockout (KO) mice was analyzed. Masson's Trichrome staining revealed obvious abnormalities in the testicular morphology of *Sema7A*$^{-/-}$ mice (Fig. 5A–F). The number of seminiferous tubules was significantly reduced in these mice compared with WT controls (Fig. 5H). In addition, the tubules displayed smaller lumina and a reduced number of spermatozoa.

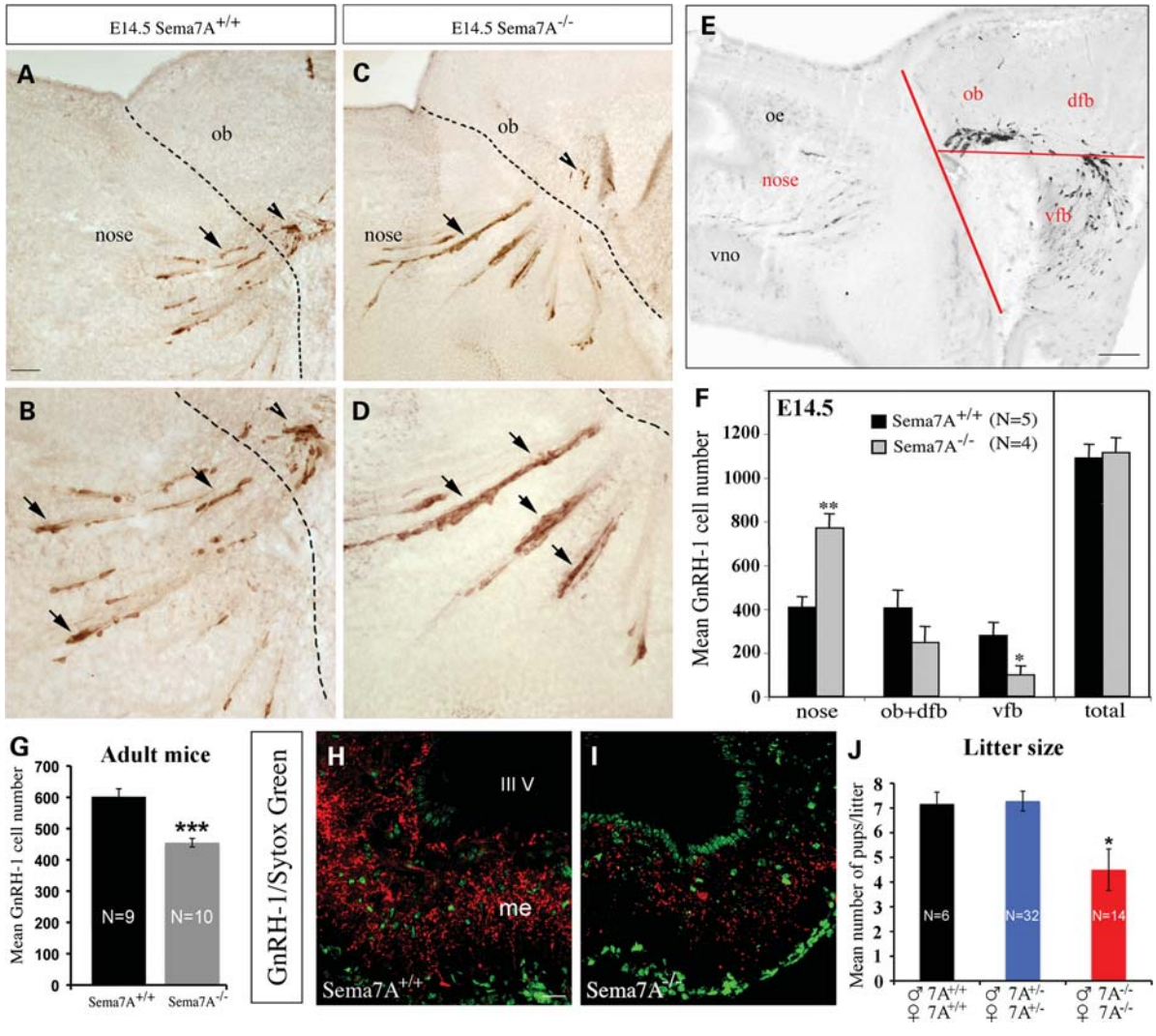

Figure 4. Defective migration of GnRH-1 cells in *Sema7A*$^{-/-}$ mice leads to altered fertility. (**A**–**D**) Photomicrographs showing GnRH-1-immunoreactivity in a sagittal section of E14.5 WT (A and B) and mutant (C and D) embryo heads. Dashed lines indicate the boundary between the nose and the forebrain (fb). Analysis of the location of GnRH-1 neurons reveals a significant accumulation of cells in the nasal region of KO mice compared with WT mice (A and B; arrows). Consistently, fewer GnRH-1 cells are located in the brain of mutant than in WT embryos (A and B versus C and D; arrowheads). (**E**) The areas of analysis for GnRH-1 neuronal location along the migratory pathway were the nasal compartment (nose), the olfactory bulb/dorsal forebrain (ob; dfb) and the ventral forebrain (vfb). (**F**) Distribution of GnRH-1 cells in each compartment of WT and mutant embryos. (**G**) Quantitative analysis of the GnRH-1 neuronal population in the brains of adult Sema7A and WT mice. (**H** and **I**) The median eminence (me) shows a dramatic loss of GnRH-1 immunoreactive terminals in mutant mice (I) compared with WT littermates (H). (**J**) Fertility in *Sema7A*$^{+/+}$, $^{+/-}$ and $^{-/-}$ female mice, mated with male mice of the same genetic background for 15 days. The number of pups per litter is significantly reduced in *Sema7A*$^{-/-}$ mice compared with WT and heterozygous controls. Data are represented as means ± SEM. $^{*}P < 0.01$; $^{**}P < 0.001$; $^{***}P < 0.0005$. Scale bars: (A and C and B and D) 50 μm and 25 μm, respectively, (E) 100 μm and (H and I) 40 μm.

Accordingly, the testes of mutants were smaller than those of WT mice (Fig. 5G).

The phenotype of *PlexinC1*$^{-/-}$ mutants was then analyzed at E14.5. The migratory process of GnRH-1 neurons was unchanged in the absence of Plexin C1, confirming that the Sema7A-dependent migratory deficit observed above is not Plexin C1-dependent (WT: $n = 3$, mean total number ± SEM = 1179 ± 78, mean number in the nasal compartment ± SEM = 480 ± 44, mean number in the olfactory bulb/dorsal forebrain ± SEM = 360 ± 20, mean number in the ventral forebrain ± SEM = 339 ± 29; *PlexinC1*$^{-/-}$: $n = 5$, mean total number ± SEM = 1089 ± 108, mean number in the nasal compartment ± SEM = 411 ± 63, mean number in the olfactory bulb/dorsal forebrain ± SEM = 371 ± 34, mean number in the ventral forebrain ± SEM = 280 ± 43; $P > 0.05$).

Sema7A promotes the migration of GN11 cells via the β1-integrin signaling pathway

The manipulation of the GnRH-1 migratory system and functional studies on these neurons have been challenging because of their limited number (800 in mice and 1000–2000 in primates) and dispersal along their migratory route. The generation of immortalized GnRH-1 neurons [NLT and GN11 cell lines; (33)] has permitted the study of more immature

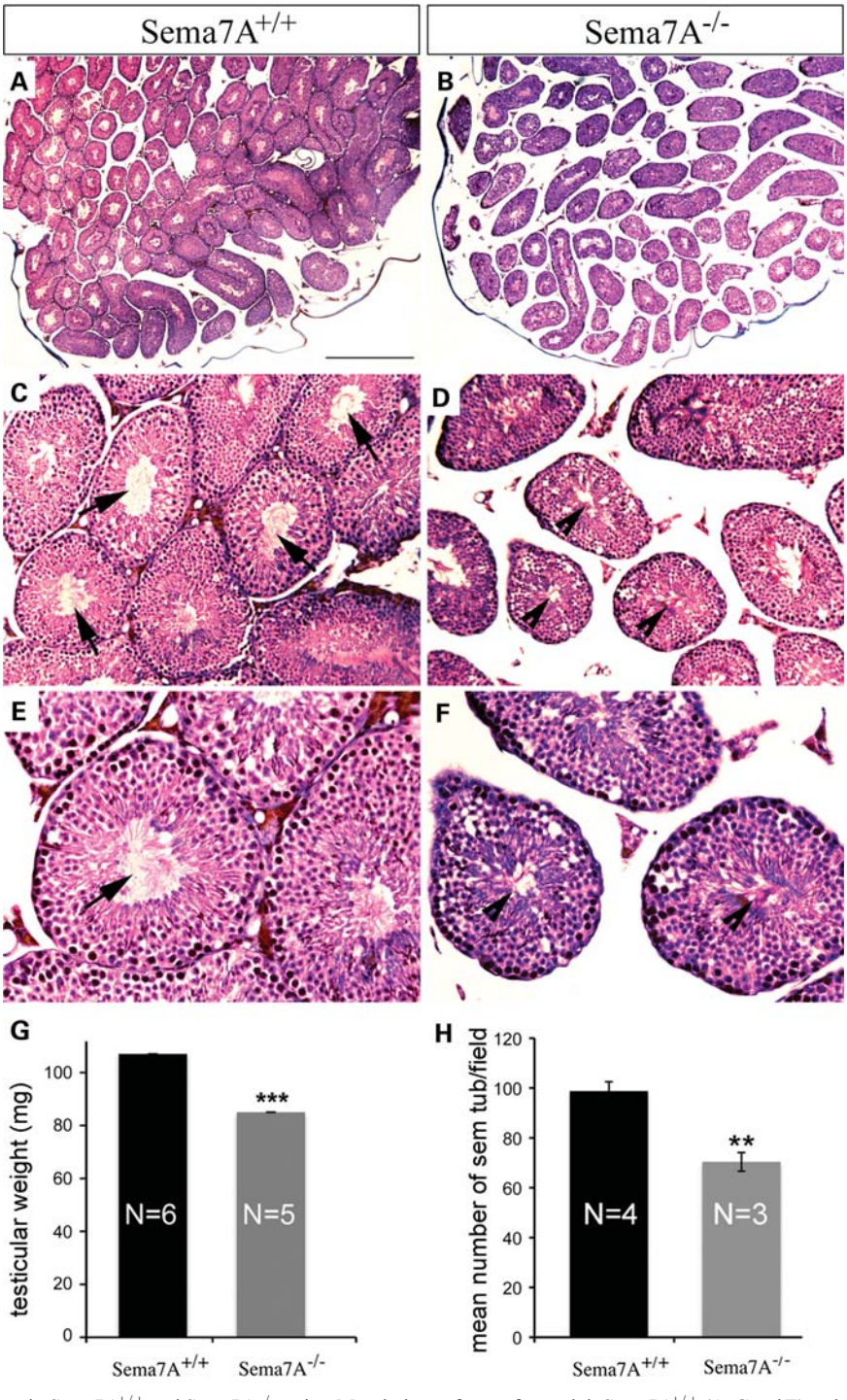

Figure 5. Testicular morphology in *Sema7A*$^{+/+}$ and *Sema7A*$^{-/-}$ mice. Morphology of testes from adult *Sema7A*$^{+/+}$ (**A**, **C** and **E**) and *Sema7A*$^{-/-}$ (**B**, **D** and **F**) mice stained by Masson's Trichrome protocol. The density of seminiferous tubules in *Sema7A*$^{-/-}$ mice is markedly reduced when compared with WTs. Seminiferous tubules in WTs (C and E) have well-developed lumina (arrows), whereas lumen formation is reduced in *Sema7A*$^{-/-}$ mice (D and F, arrowheads), with fewer spermatozoa and an accumulation of immature spermatogenic cells. (**G**) Testicular weight (mg) in control and *Sema7A*$^{-/-}$ mice, showing a significant reduction in the latter. Values represent means ± SEM. $^{**}P < 0.005$; $^{***}P < 0.0005$. Scale bars: (A and B) 400 μm, (C and D) 100 μm and (E and F) 50 μm.

migratory neurons. In particular, GN11 cells display remarkable motility *in vitro*, and have been used to investigate the molecular mechanisms controlling the directional migration of GnRH-1 neurons and to shed light on the biochemical pathways employed by GnRH-1 cells (8,10,34).

To assess whether GN11 cells could be used for functional studies of Sema7A, RT-PCR (Fig. 6A) and western blot analysis (Fig. 8C) were carried out to verify the expression of Sema7A receptors. β1-Integrin, but not Plexin C1, was detected in GN11 cells (Fig 6A). The non-receptor protein

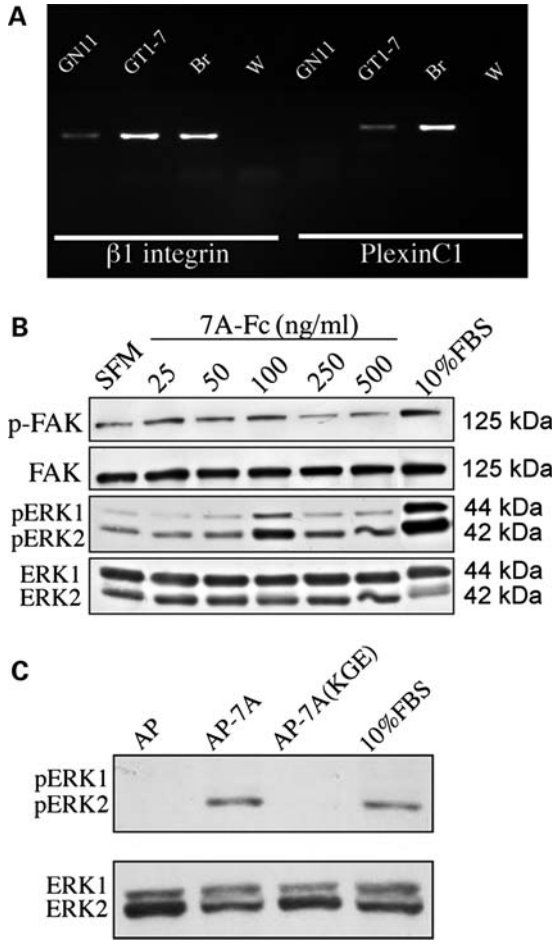

Figure 6. Sema7A activates the β1-integrin/MAPK pathway and increases the motility of GN11 cells. (**A**) RT-PCR for β1-integrin and Plexin C1 was performed on total RNA isolated from the indicated cells. Positive (postnatal brain; Br) and negative controls (water; W) were included in the reaction mix. (**B**) Sema7A stimulates the phosphorylation of FAK and MAPK. Cells were treated with different doses of recombinant Sema7A or 10% FBS (positive control) for 15 min and controls were treated with vehicle. Total cell lysates were resolved on 10% SDS–PAGE and subjected to immunoblotting with the indicated antibodies. (**C**) GN11 cells were treated with AP-, AP-Sema7A- or AP-7A-KGE-conditioned medium (20 nM) and 10% FBS for 15 min, and subjected to immunoblotting with antibodies specific for the phosphorylated forms of ERK1 and ERK2 and total ERK1/ERK2. Experiments were done in triplicate with similar results. Stimulation with AP-Sema7A induces an increase in the phosphorylation of MAPK, whereas treatment with AP-7A-KGE does not lead to the activation of ERKs.

tyrosine kinase focal adhesion kinase (FAK) plays a central role in β1-integrin-dependent signaling (22), being rapidly phosphorylated upon ligand binding and leading to the activation of the cytoskeletal components responsible for signal transduction downstream of the integrins. To determine whether Sema7A induces integrin-dependent signaling responses, GN11 cells were treated for 15 min with recombinant Sema7A protein, and FAK- and extracellular signal-regulated kinases 1/2 (ERK1/2)-phosphorylation subsequently assessed. Sema7A activated FAK in a dose-dependent manner, with maximum activation at 100 ng/ml that decreased at higher doses (Fig. 6B). ERK1/2 displayed the same phosphorylation kinetics. To assess whether the conditioned medium (CM) of 293T cells transiently transfected with AP (alkaline-phosphatase)-Sema7A also induced MAPK activation, GN11 cells were treated with AP-, AP-Sema7A- and AP-Sema7A(KGE)-conditioned media, after which the phosphorylation of ERK kinases was determined. Sema7A(KGE) is a Sema7A mutant in which the putative integrin-binding RGD sequence has been mutated to KGE, which is not recognized by integrins (22). AP-Sema7A caused a significant increase in ERK phosphorylation, whereas AP-Sema7A(KGE) had no effect (Fig. 6C). Our results thus show that this activation is most likely dependent on β1-integrin binding.

To determine how Sema7A regulates the migration of GN11 cells, we carried out time-lapse video microscopy of cells migrating into a scratch wound for 12 h under different conditions (Fig. 7; $n = 4$ for each condition). Exposure to AP-Sema7A increased the migration of the cells, resulting in shorter healing times (Fig. 7D–F) than in controls (Fig. 7A–C) and in AP-Sema7A(KGE)-treated cells (Fig. 7G–I). Furthermore, an analysis of the area covered by migrating cells revealed a significant increase following AP-Sema7A stimulation but not after treatment with AP alone or Sema7A(KGE)-AP conditioned media (Fig. 7J). Since Sema7A is highly expressed along the developing olfactory axonal scaffold, experiments were performed comparing soluble versus adherent forms of Sema7A. Cell migration was significantly promoted under both conditions (Fig. 7J and K). Finally, single-cell tracking was performed using dissociated GN11 cells treated with soluble CM (Fig. 7L and M) or directly plated onto CM-coated dishes (Fig. 7N and O). Both soluble and adherent forms of Sema7A significantly induced directional cell movement when compared with other treatments (Fig. 7M and O). GN11 cells treated with AP alone or AP-Sema7A(KGE) moved in different directions randomly, whereas AP-Sema7A-treated cells tended to migrate in the same direction and traveled farther distances from their point of origin (Fig. 7L and N). Differences in migration patterns were quantified by comparing migratory persistence, calculated as the ratio of the linear distance from the starting point of each recording to the end point to the total distance traversed by the cell (35). Treatment with either soluble or adherent AP-Sema7A induced a significant increase in persistence when compared with AP alone or AP-Sema7A(KGE) (Fig. 7M and O).

We hypothesized that Sema7A could trigger directional migration by increasing β1-integrin-dependent adhesion. To test this hypothesis, the effect of Sema7A on cell adhesion of GN11 cells plated on a β1-integrin-specific adhesive substrate, fibronectin (FN), was examined (Fig. 8A and B). Different doses of recombinant Sema7A induced a significant increase of cell adhesion of GN11 cells on FN-coated surfaces (Fig. 8A) and this increase was β1-integrin dependent, since it was inhibited by the monoclonal antibodies BMA5 and Ha2/5, which block α5β1 and β1 integrins, respectively (Fig. 8B).

To study the migratory behavior of GnRH-1 neurons when encountering a Sema7A substrate that imitates the semaphorin-rich olfactory fibers, GN11 cells were used in a modified wound-healing assay which employed coated-stripes (50 μm wide) of AP-Sema7A (red stripes), alternating with AP-Sema7A(KGE)-substrate (gray stripes), as an internal control (Supplementary Material, Video S1). Cell

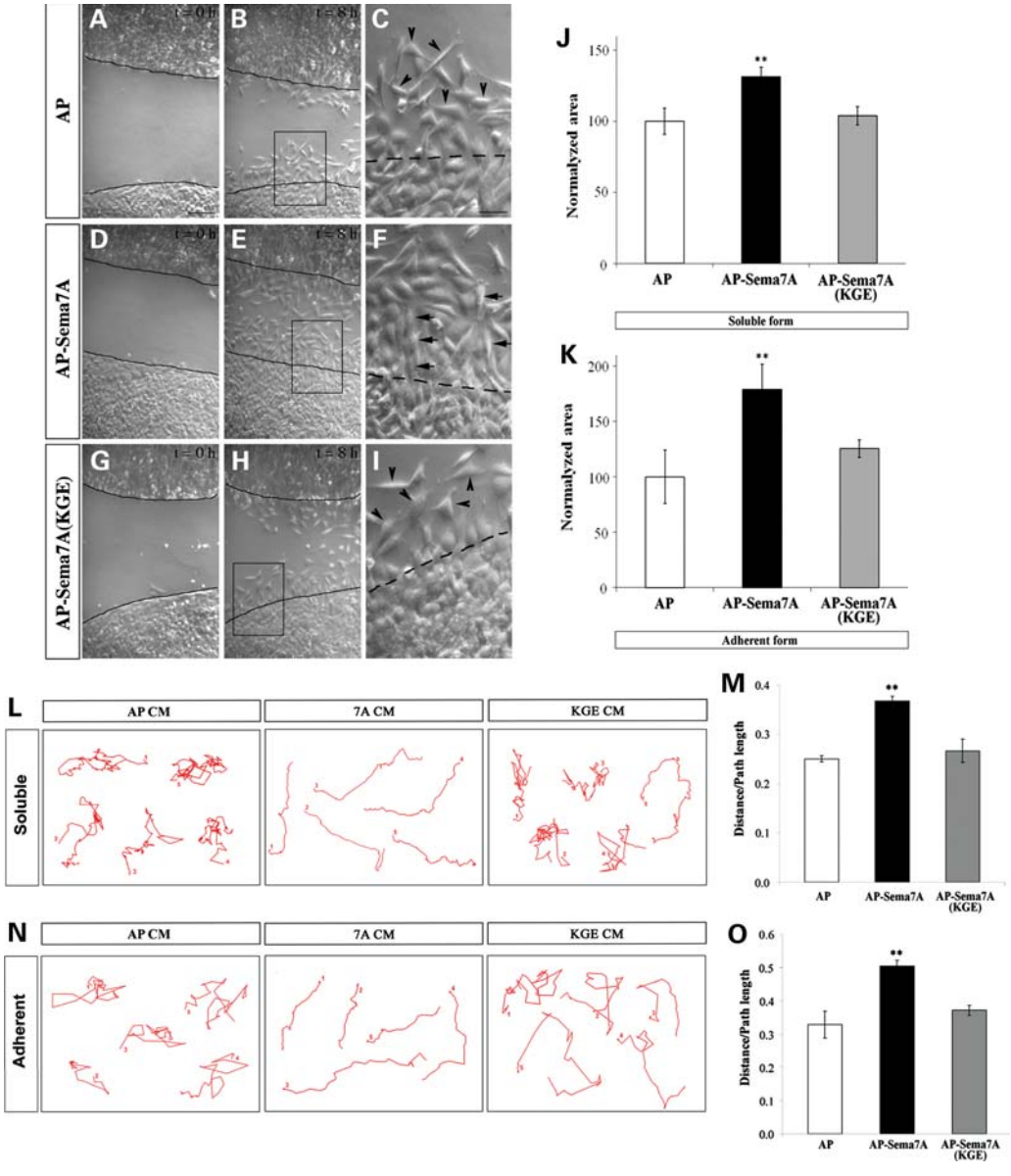

Figure 7. Sema7A regulates integrin-mediated GN11 cell migration by increasing directional persistence. (**A**–**I**) Representative photomicrographs of wound-healing assay performed on GN11 cells treated with soluble AP-Sema7A-, AP-Sema7A-KGE- or AP-conditioned media. Continuous lines indicate the borders of the wound at the initial recording time. (C–I) High-power view of boxed areas depicted in (B), (E) and (H). In the presence of Sema7A (D, E and F), GN11 cells tend to move more uniformly, in a proximal-to-distal direction (arrows), compared with other conditions in which cells move at random to occupy wound sites (C and I, arrowheads). (**J**) Quantification of the area occupied by cells under soluble protein treatment. (**K**) Quantification of the area (normalized to controls) occupied by cells adhering to the indicated substrates. Quantitative data are means ± SEM ($n = 4$) and normalized to control conditions. (**L** and **N**) Representative examples of GN11 cell tracks after treatment with soluble (L) and adherent (N) Sema7A, Sema7A(KGE), or CM with empty vector-transfected cells (AP, alkaline phosphatase). GN11 cells were recorded by time-lapse video microscopy for at least 3 h. The movement of individual cells was followed using the cell-tracking software (ImageJ) and different cell migration parameters were measured (**M** and **O**). Persistence of each cell was calculated using at least 140 tracks pooled from three separate recordings. Data are means ± SEM ($n = 3$). ANOVA followed by Tukey's HSD *post hoc* analysis was used to compare groups. $^{**}P < 0.01$. Scale bars: (A, B, D, E, G and H) 30 μm, and (C, F and I) 10 μm.

migration on the striped substrate was recorded using time-lapse imaging for 6 h after wound formation. In these studies, GN11 neurons which grew onto Sema7A-coated stripes covered more distance when compared with KGE-coated substrate as a consequence of a more polarized migrational behavior and increased directionality (Supplementary Material, Video S1).

Finally, we asked whether the observed dynamic *in vivo* expression of Plexin C1 would allow regulating the migratory behavior of GnRH-1 cells in response to Sema7A. In order to address this question, the migration of GN11 cells over-expressing Plexin C1 was investigated (Fig. 8C and D). In a transwell system, mock-transfected GN11 cells showed greater locomotion in response to 100 ng/ml of Sema7A

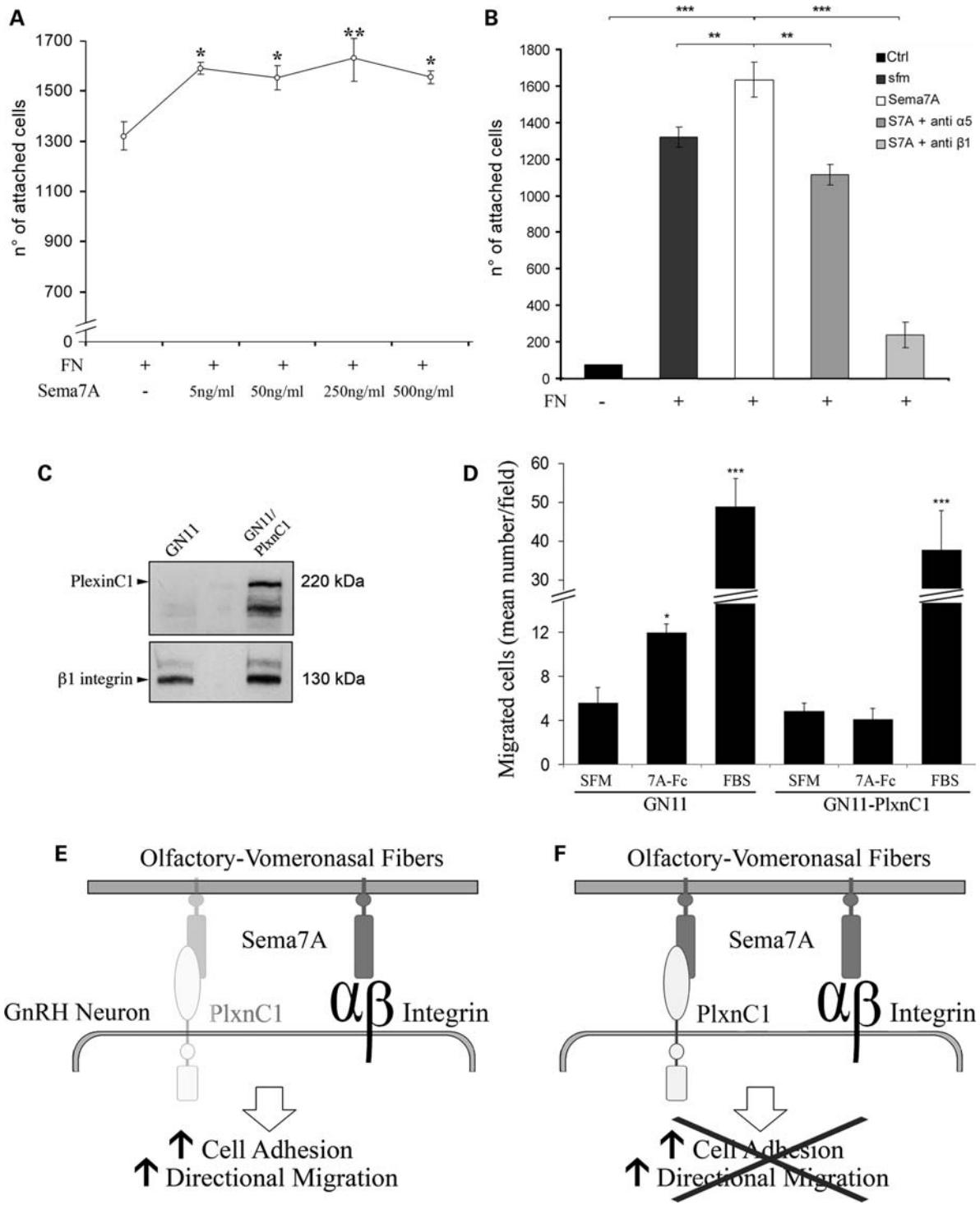

Figure 8. Sema7A triggers GN11 directional migration by increasing β1-integrin-dependent adhesion. (**A** and **B**) Recombinant Sema7A regulates integrin-mediated adhesion. (A) Cell adhesion on FN-coated surfaces of GN11-treated cells with various concentration of recombinant Sema7A. (B) Cell adhesion of GN11 cells on control (BSA) or FN treated or not with 250 ng/ml Sema7A, in the presence or absence of neutralizing antibodies against α5β1 or β1 integrins. (**C**) Western blot analysis for Plexin C1 and β1-integrin performed on total cell lysates from WT and Plexin C1-overexpressing GN11 cells. (**D**) GN11 migration was analyzed in a transwell assay in the presence or absence of recombinant Sema7A (100 ng/ml). Mock-transfected GN11 cells significantly increase their migration in the presence of Sema7A and 10% FBS, whereas Plexin C1-transfected GN11 cells do not respond to Sema7A stimulation. (**E** and **F**) Schematic illustrations of the novel aspects of Sema7A signaling uncovered in this study. (E) Sema7A is expressed along the developing olfactory/vomeronasal axons and acts on GnRH-1 neurons increasing adhesion and persistent migration through β1-integrin binding and activation. (F) Expression of Plexin C1 in GnRH-1 neurons switches off their migratory response to Sema7A. Data are mean ± SEM ($n = 3$ for A and B and $n = 12$ for D). ANOVA followed by Fisher's LSD *post hoc* analysis was used to compare groups. $^{*}P < 0.05$; $^{**}P < 0.01$; $^{***}P < 0.001$.

(Fig. 8D) and 10% fetal bovine serum (FBS) (positive control) when compared with serum-free medium (SFM). However, the over-expression of Plexin C1 by these cells completely abolished Sema7A-induced migration (Fig. 8D).

Taken together, these data demonstrate that Sema7A positively modulates both cell adhesion and persistent migration of GN11 cells in a β1-integrin-dependent manner, whereas expression of Plexin C1 switches off their migratory response to Sema7A (Fig. 8E and F).

DISCUSSION

The regulation of reproductive function in mammals is mediated by the pulsatile secretion of GnRH-1 from the hypothalamus. Alterations in the migratory process of GnRH-1 neurons lead to defective GnRH-1 secretion and, subsequently, to reproductive deficits. The complex developmental events leading to correct GnRH-1 neuronal migration are tightly regulated by specific spatiotemporal expression patterns of growth factors, adhesion molecules and diffusible attractants and repellents (1,7).

Sema7A is expressed along the GnRH-1 migratory route during mouse embryonic development, with high levels in the nasal pit, where these cells start their migratory process, and along the olfactory/vomeronasal axonal scaffold. *Sema7A*$^{-/-}$ mice show deficits consistent with the reduced migration of GnRH-1 neurons, and the lack of olfactory axonal abnormalities in *Sema7A*$^{-/-}$ mice suggests that the alteration of Sema7A signaling leads to an isolated deficit in GnRH-1 neuronal migration without affecting the olfactory system. Since other semaphorins are known to be expressed in this structure during development (9,36–42), the lack of a strong olfactory phenotype in the KO mice could also suggest that other redundant semaphorin-signaling pathways guarantee the establishment of the olfactory/vomeronasal systems. We and others have indeed previously shown that at least three semaphorins (i.e. Sema4D, Sema3A and Sema3F) are present in the developing nasal region and, in particular, class-3 semaphorins control the correct targeting of the olfactory and vomeronasal axons into the developing brain (8–10,36,37,40,42).

In the brains of adult *Sema7A* mutant mice, the population of GnRH-1 cells is significantly reduced by approximately a third compared with WT littermates. It is important to emphasize that in recent years, there has been extensive documentation of a high degree of heterogeneity within the GnRH-1 neuronal population. It is therefore unlikely that a single genetic mutation could completely prevent these neurons from reaching their destination. The failure of puberty in mammals might occur only when the majority of GnRH-1 neurons are affected by mutations in multiple genes (43,44).

It is possible that in *Sema7A*$^{-/-}$ animals, GnRH-1 cells that do not reach their target areas at the right time are eliminated by cell death. However, due to the small size of the GnRH-1 neuronal population and the limited temporal window during which apoptosis takes place, it is not possible to determine whether this is the case. The loss of GnRH-1 immunoreactive neurons has also been reported in other mutant mice, such as *neuropilin2*$^{-/-}$, *netrin1*$^{-/-}$ and *ephrin3–5*$^{-/-}$ mice, but its cause remains undetermined (8,45,46). Alternatively, the reduction of GnRH-1 neurons in the mutants' brains could result from a deficit of the migratory process. As a matter of fact, in these mice, GnRH-1 neurons accumulated in the nasal compartment at E14.5, resulting in approximately twice as many GnRH-1 cells as in WT mice. A previous work has shown that the mutation of *Prok2*, one of the genes mutated in autosomal forms of KS, severely reduces the number of GnRH-1 neurons in the adult hypothalamus, and GnRH-1 cells were found to be trapped in close proximity of the cribriform plate at E13.5 (47).

As a result of the reduced number of GnRH-1 cells in the brain of *Sema7A*$^{-/-}$ mice, the median eminence of these mice also appears to be more sparsely innervated by GnRH-1 fibers than in WT mice. These observations together with the reduction in the size of the litters are consistent with a compromised GnRH-1 system. Thus, it appears that the lack of Sema7A signaling during development initiates a sequence of events that leads postnatally to the suboptimal maturation of the GnRH-1 network and an impaired ability to produce offspring. Further studies will be required to assess whether it is the female, the male or both null mice carrying these fertility problems.

The male gonads show striking defects in the adult mutant mice; however, we cannot exclude the possibility that these defects could also be partially due to other peripheral indirect effects occurring during development at the level of the testes. We are currently not aware whether Sema7A is expressed at these sites during embryonic development; however, previous findings revealed robust Plexin C1 mRNA expression in the mice sex cords, which later develop into seminiferous tubules (48).

The expression pattern of the two Sema7A receptors in GnRH-1 neurons appears to be spatiotemporally regulated: at early stages of their migratory route, GnRH-1 neurons only express β1-integrin receptor, whereas they begin to express Plexin C1 during subsequent developmental stages and at anatomical sites at which these cells stop migrating (ventral forebrain). There is accumulating evidence to show that semaphorin signaling is multifaceted, and that these molecules can regulate integrin function, cell adhesion and migration both negatively and positively, depending on the cellular context and on the subsets of receptors expressed (12,49).

Biochemical analysis indicates that Sema7A at low doses stimulates the rapid phosphorylation of FAK and ERK1/2 in GN11 cells. The phosphorylation of FAK, which occurs upon integrin activation, is consistent with Sema7A, increasing the directional migration of these cells in a β1-integrin-dependent manner. Our *in vivo* results indicated that the migratory process of GnRH-1 neurons in E14.5 *Plexin C1*-null mice was unchanged when compared with WT mice, strengthening the importance of Sema7A-β1-integrin signaling during this stage. The functional *in vitro* experiments demonstrate that Sema7A modulates motility of GN11 cells by increasing their directional migration engaging β1-integrin-dependent adhesion. Membrane-bound Sema7A expressed by guidepost olfactory axons could thus modulate the response of GnRH-1 neurons to local cues, by promoting integrin-based cell adhesion and

the directional movement of these neurons toward the forebrain, finally leading to a more efficient cell migration.

Plexin C1 overexpression in GN11 cells completely abolished Sema7A-induced migration, indicating that Sema7A plays a dual role in the regulation of cell motility via the differential activation of β1-integrin and Plexin C1, with the former promoting enhanced directional migration in response to chemotropic molecules, and the latter attenuating this response. Indeed, previous studies have shown that Plexin C1 signaling in melanocytes inhibits β1-integrin-dependent attachment and spreading in response to Sema7A (18). This implies that a similar mechanism could also exist in the GnRH-1 system.

The data presented in this report promote our understanding of the molecular mechanisms controlling the development of the GnRH-1 and reproductive systems and may help to elucidate the etiology of some forms of IHH. This human disease is genetically heterogeneous, with several associated loci that account for ∼40% of all cases (4). The genes involved encode proteins essential for the development of GnRH-1 neurons and the secretion and activity of the neuropeptide (43,50–52), and the clinical features of GnRH-1 deficiency are likely to be a result of the involvement of multiple genetic defects. Interestingly, according to a recent report, mutations in genes involved in IHH were also associated with hypothalamic amenorrhea (6), and all six mutations identified were found to be heterozygous in these patients. The authors speculate that such heterozygous mutations, although not sufficient to cause IHH, could set a lower threshold for the functional inhibition of the hypothalamic–pituitary–gonadal axis and thereby lead to other reproductive dysfunctions. To our knowledge, mutations in semaphorins-associated genes have not been investigated so far in IHH-affected individuals. The present study, together with previous works (8–10), strongly indicates the relevance of these molecules in the development of the GnRH-1 system and provides important data for future genetic studies that could shed light into the etiology of some reproductive defects.

In summary, we provided insights into the molecular basis of semaphorin-dependent signaling in the correct establishment of the GnRH-1 and reproductive systems. Lack of this signaling pathway impairs the final size of the GnRH-1 neuronal population in the hypothalamus, leading to altered fertility. It also has wider biological significance, as our results uncover a novel role for Sema7A-β1-integrin signaling in the regulation of neuronal migration.

MATERIALS AND METHODS

Animals

Experiments were conducted in accordance with current European Union and Italian regulations, under the authorization of the Italian Ministry of Health, No. 66/99-A, and in accordance with National Institutes of Health (NIH)/National Institute of Neurological Disorders and Stroke guidelines, and Animal Care and Use Committee approval. CD-1 embryos or NIH Swiss embryos were harvested at E11.5, E12.5 and E14.5 (plug day, E0.5) and used for nasal explants, or fixed overnight at 4% PFA in 0.1 M phosphate buffer, pH 7.4, cryoprotected and frozen and stored (−80°C) until processing for immunohistochemistry. For *in situ* hybridization experiments, E11.5 and E12.5 embryos were directly frozen and sections cut on a cryostat. *Sema7A*$^{-/-}$ and *Plexin C1*$^{-/-}$ mice have been previously characterized (22).

Adult mice (3–5 months old) were anesthetized with an intraperitoneal injection of 200 mg/kg ketamine and perfused with 4% PFA.

Histology of the testes

Testes were collected from 3-month-old *Sema7A*$^{+/+}$ and *Sema7A*$^{-/-}$ mice, fixed in 4% PFA solution and stored at 4°C. Paraffin-embedded testes were sectioned at a thickness of 5 μm (histology facility, University of Lille 2, France) and stained using Masson's Trichrome protocol.

Immunohistochemistry

Tissues were cryosectioned (Leica cryostat) at 16 μm intervals in the case of embryos, and at 35 μm intervals for free-floating sections in the case of adult brains. Immunohistochemistry was performed as previously reported (10,30). For immunofluorescence, Alexa-Fluor 488 (1:400)- and Cy3- (1:800)-conjugated secondary antibodies (Invitrogen, Molecular Probes) were used. Fluorescent specimens were mounted using 1,4-diazabicyclo[2.2.2]octane (DABCO; Sigma-Aldrich).

The primary antisera used were as follows: rabbit anti-GnRH-1: LR1 (1:8000 and 1:4000 for immunofluorescence; kindly provided by Dr Benoit, Montréal, Canada) and guinea pig anti-GnRH-1 (1:1000, a generous gift of Dr Philippe Ciofi, Neurocentre Magendie, Inserm U862, Bordeaux, France); goat anti-Plexin C1 (N-17) (1:50): sc-10149 (Santa Cruz Biotechnology, Inc.); rabbit anti-β1-integrin (M-106) (1:20): sc-8978 (Santa Cruz Biotechnology, Inc.); rabbit anti-Peripherin (1:1000): AB1530 (Chemicon, Temecula, CA, USA); rabbit anti-Sema7A (1:50): ab23578 (Abcam); goat anti-Sema7A (1:100): sc-67969 (Santa Cruz Biotechnology, Inc.); mouse anti-β-tubulin (1:500) (Sigma-Aldrich).

In situ hybridization

Non-radioactive *in situ* hybridization was carried out with digoxigenin-labeled antisense cRNA probes transcribed from rat *Sema7A* (a 362 bp fragment corresponding to nucleotides 364–726 of the coding region) (24). The generation of cRNA probes and the *in situ* hybridization protocol were as described previously (53).

Image analysis

Images were captured using a microscope (Eclipse 80i; Nikon) with 2×/0.06 NA, 10×/0.30 NA and 20×/0.50 NA objectives (Nikon) and equipped with a digital camera (CX 9000; MBF Bioscience). For confocal observations and analyses, an inverted laser scanning Axio observer microscope (LSM 710, Zeiss) with EC Plan NeoFluor 10×/0.3 NA, 20×/0.5 NA and 40×/1.3 NA (Zeiss) objectives were used (Imaging Core Facility of IFR114 of the University of Lille 2, France).

ImageJ (National Institute of Health, Bethesda, USA) and Photoshop CS4 (Adobe Systems, San Jose, CA, USA) were used to process, adjust and merge the photomontages.

Nasal explants

Nasal explants were generated as previously described (28). Briefly, the nasal pits of E11.5 NIH Swiss mice were isolated under aseptic conditions in Gey's Balanced Salt Solution (Invitrogen) enriched with glucose (Sigma-Aldrich), and maintained at 4°C until plating. Nasal explants were placed onto glass cover slips coated with 10 μl of chicken plasma (Cocalico Biologicals, Inc.). Thrombin (10 μl; Sigma-Aldrich) was then added to allow the explant to adhere to the cover slip (thrombin/plasma clot). Explants were maintained in defined SFM containing 2.5 mg/ml fungizone (Sigma-Aldrich) at 37°C with 5% CO_2 for up to 30 DIV. From culture day 3 to day 6, fresh media containing fluorodeoxyuridine (8×10^{-5} M; Sigma-Aldrich) was provided to inhibit the proliferation of olfactory neurons and non-neuronal tissue. The medium was replaced by fresh SFM twice a week.

Single-GnRH-1 cell isolation

Cell isolation and single-cell RT-PCR were performed as previously described (30). Briefly, nasal explants were washed twice with 1× PBS (without Mg^{2+} or Ca^{2+}). Single-GnRH-1 cells were identified by their bipolar morphology, association with outgrowing axons, and location, and then isolated from nasal explants using a micropipette controlled by a micromanipulator (Narishige) connected to an inverted microscope (IX51; Olympus) at four time points (3, 4, 10 and 28 DIV). Cells isolated at 3 and 4 DIV are representative of migratory GnRH-1 cells, whereas cells at 10 and 28 DIV are post-migratory neurons. cDNA was generated and PCR amplification performed as described previously (54).

Microarray and data analysis

Microarray experiments on GnRH-1 cells and midline nasal cartilage were performed previously in the laboratory of Dr Susan Wray (Cellular and Developmental Neurobiology Section, NINDS Porter Neuroscience Research Center, Bethesda, MA, USA) using material obtained from single-GnRH-1 cells (32,54) and midline nasal cartilage. All material was subsequently processed (labeled and hybridized) by the DIRP NIH microarray core facility. GeneChip Mouse Genome 430 2.0 arrays (Affymetrix, Santa Clara, CA, USA) were used. The microarrays were checked for noise and outliers using custom R scripts, including covariance-based PCA, correlation heat maps, LOWESS analysis, and clustering. The data were normalized such that the average expression of genes in all chips was similar, log-transformed and statistical analysis carried out using Student's *t*-test. Since levels of receptors were generally an order of magnitude lower than those of housekeeping genes, receptor expression was analyzed after grouping in order to distinguish positive signals from background. Genes were filtered on the basis of call, fold-change and *P*-value. In this report, the Sema7A receptors Plexin C1 and β1-integrin were examined. Genes with a signal log ratio greater than ± 0.5 (1.41-fold) and a *P*-value <0.05 were chosen as being statistically different.

To investigate which pathways the Sema7A receptors map to in GnRH-1 cells, and to determine whether there are interactions between them, the data set containing gene identifiers along with the corresponding fold changes was uploaded into the Ingenuity Pathways Analysis program. A 1.41-fold change (log ratio ± 0.5) was set to identify genes whose expression was significantly differentially regulated. Networks of these focus genes were then algorithmically generated based on their connectivity. All interactions were supported by at least one reference from the literature or from canonical information stored in the Ingenuity knowledge base.

Analysis of GnRH-1 neurons in transgenic mice

Serial sagittal sections (16 μm thickness) from E14.5 *Sema7A*$^{-/-}$ ($n = 4$), *Plexin C1*$^{-/-}$ ($n = 5$) and WT mice (*Sema7A*$^{+/+}$, $n = 5$; *Plexin C1*$^{+/+}$, $n = 3$) were cut and immunolabeled for GnRH-1 and peripherin. A quantitative analysis of GnRH-1 neuronal number as a function of location was performed, with GnRH-1 cells being counted in three regions (the nasal compartment, olfactory bulb/dorsal forebrain and ventral forebrain). Serial coronal sections (35 μm, six series) from adult *Sema7A*$^{-/-}$ (females, $n = 5$; males, $n = 5$) and *Sema7A*$^{+/+}$ mice (females, $n = 5$; males, $n = 4$) were labeled for GnRH-1. Total numbers of GnRH-1 cells were calculated for each brain and combined to give group means ± SEM.

Cell cultures

All cell lines were grown in monolayers at 37°C under 5% CO_2, in DMEM (Invitrogen) containing 1 mM sodium pyruvate, 2 mM glutamine (Invitrogen), 100 μg/ml streptomycin, 100 U/ml penicillin and 4500 mg/500 ml glucose (MP Biomedicals), supplemented with 10% FBS (Invitrogen) as previously described (10). The medium was replaced at 2-day intervals. Subconfluent cells were routinely harvested by trypsinization and seeded onto 58 cm^2 dishes (1×10^5 cells). GN11 cells were always used for experiments between their third and sixth passages.

In vitro cell transfection

293T cells were transiently transfected using the fast-forward protocol. Briefly, a 58 cm^2 subconfluent dish was split into four dishes in OptiMEM medium (Invitrogen) about 1 h before high-efficiency liposome transfection (Lipofectamine 2000, Invitrogen). Each dish was transfected with 2–4 μg of DNA construct (recombinant Sema7A fused to AP, AP only and Sema7A-KGE). Sema7A-KGE is a mutated form of Sema7A, in which the putative integrin-binding RGD sequence is altered to KGE (22). GN11 cells were transfected using the same protocol with a construct encoding the full-length form of Plexin C1 (22).

Transwell assay

Transwell experiments were performed following protocols previously described (55). Briefly, GN11 cells (1×10^4 cells) were seeded onto the upper side of 8 μm-pore filters in transwell chambers (Falcon) and incubated overnight in serum-free DMEM with or without recombinant Sema7A (R&D Systems) in both chambers ($n = 12$ for each treatment condition). Cells on the upper side of the filters were then mechanically removed. GN11 cells from the lower side of the filter were then fixed in cold 100% methanol for 5 min, and the nuclei stained with DAPI.

Western blot analysis

For phosphorylation experiments, subconfluent GN11 cells were grown overnight in SFM and then stimulated with SFM or recombinant Sema7A protein (R&D Systems) at the indicated concentration for 15 min. Stimulation with Sema7A fused with AP (Sema7A-AP), AP only or Sema7A-KGE-AP was performed using conditioned medium diluted 1:3 for 15 min. Western blot experiments were performed as previously described (10).

The primary antibodies used were as follows: 1:1000 mouse anti-phospho-ERKs (Cell Signaling Technology) and 1:1000 rabbit anti-ERKs (Cell Signaling Technology); 1:1000 mouse anti-phospho-FAK (Santa Cruz Biotechnology, Inc.) and 1:1000 mouse anti-FAK (Santa Cruz Biotechnology, Inc.); 1:200–1:500 goat anti-Plexin C1 (N-17; Santa Cruz Biotechnology, Inc.); 1:100–1:500 rabbit anti-β1-integrin (M-106; Santa Cruz Biotechnology, Inc.); 1:30 000 mouse anti-α-actin (Sigma-Aldrich).

Single-cell tracking

For single-cell tracking experiments, GN11 cells were seeded at low density (3×10^3 cells/cm^2) into culture dishes in complete medium (serum-free DMEM containing 1 mM sodium pyruvate, 2 mM glutamine, 100 μg/ml streptomycin, 100 U/ml penicillin and 9 mg/ml glucose) with or without recombinant Sema7A (either in the soluble form or in the adhesive form) from conditioned media, and cell migration was analyzed by time-lapse video microscopy for at least 3 h.

Wound-healing assay

GN11 cells were seeded at a high density (1.25×10^5 cells/cm^2) into cell culture insert (ibidi) to generate a wound with a gap of 500 μm. After overnight incubation, the medium was replaced by conditioned media and cell migration was analyzed by time-lapse video microscopy for a duration of 8 h. The area occupied by migrating GN11 cells was measured using ImageJ software and normalized to controls.

Time-lapse video microscopy

Cells were kept at 37°C under 5% CO_2 in an incubator chamber for time-lapse video recording (Okolab). Cell movements were monitored with an inverted microscope (Eclipse Ti, Nikon) using 4×/0.10 or 10×/0.25 NA Plan objectives. Images were collected with CCD video cameras (Roper Scientific) at 3–5 min time intervals, digitized and stored as image stacks using the MetaMorph 7.6.1.0 software (Universal Imaging Corp.). Image stacks were analyzed with the NIH image software (ImageJ) and at least 100 cells per treatment/condition were manually tracked using MtrackJ plugin. Cells whose migration was not contained within the image field for the duration of the experimental run, as well as cells that divided, were excluded from this calculation. The velocity of each cell was calculated by dividing the accumulated distance from the starting point to the final position of the cell path by the time elapsed. To discriminate between random and directional migration, the Euclidean distance from the starting point to the final position of the cell (i.e. the vectorial distance traversed) was divided by the accumulated distance (total path length). This value was multiplied by the square root of the cell track duration. For wound-healing experiments, images were obtained every 5 min for a duration of 8 h and the area occupied by migrating GN11 cells was measured using the ImageJ software. Data were normalized to the free area at the first time point ($t = 0$) and then to controls.

Adhesion assay

For adhesion assay, 2×10^4 GN11 cells were resuspended in 0.1 ml of SFM containing increasing doses of recombinant Sema7A (R&D Systems) with or without anti-α5β1-integrin (BMA5, Millipore; 20 μg/ml) or anti β1-integrin (BD Pharmigen; 25 μg/ml) blocking function antibodies, plated on Millicoat™ Cell Adhesion Strip (Millipore)-coated FN, incubated for 30 min at 37°C, washed three times with PBS and stained with 0.2% crystalviolet, 10% ethanol.

Stripe assay

To obtain a surface alternatively coated with Sema7A and Sema7A-KGE, stripes were prepared following a modified version of the stripe assay protocol described by Knöll *et al.* in 2007 (56). Briefly, two different solutions were prepared using 20-fold concentrated Sema7A or Sema7A-KGE CM supplemented, respectively, with CY3-conjugated or unconjugated dextran. In the first step, Sema7A solution was injected into the inlet channel of 50 μm-wide parallel channel silicon matrix (Max Plank Institute, Tübingen, Germany) and incubated for 2 h at 37°C in a humidified incubator. Then the matrix was removed and, after three washes with bi-distilled sterile water, the Sema7A-KGE mix was added on the entire surface and incubated for 2 h. Stripes were finally washed three times again and air-dried under sterile condition. To obtain a linear cell front orthogonal to the stripes, GN11 cells were seeded at a high density (1.25×10^5 cells/cm^2) in cell culture insert (ibidi) in close proximity to the stripes.

Statistical analysis

For the comparison of multiple groups, statistical significance was determined using a two-way analysis of variance (ANOVA; for Gaussian distributed data) followed by Tukey's HSD *post hoc* analysis or Kruskal–Wallis (non-parametric) tests. For comparisons between paired,

normally distributed data, a paired *t*-test was used. A *P*-value <0.05 was considered to indicate a significant difference. Data are indicated as means $\pm$ SEM per group (for normally distributed data). A non-parametric unpaired test (Wilcoxon–Mann–Whitney) was used to compare the percentages of primary GnRH-1 cells expressing specific transcripts at different *in vitro* stages. A *P*-value <0.01 was considered to indicate a significant difference.

SUPPLEMENTARY MATERIAL

Supplementary Material is available at *HMG* online.

ACKNOWLEDGEMENTS

We thank Dr N. Sharifi, Ms A. Reuss and Ms J. Lee (former members of CDNS) for the generation of the single-GnRH-1 cell cDNAs and midline tissue used for microarray screening, Dr A. Elkahloun (DIRP NIH Microarray Core Facility) for the labeling and hybridization of microarray material, Dr K. Johnson (DIRP NIH Microarray Core Facility) for analyzing microarray data, Miss Meryem Tardivel of the Imaging Core Facility of IFR114 of the University of Lille 2 for technical assistance, Mr Julien Devassine (animal facility of the JPARC, University of Lille 2) for the maintenance of transgenic mouse lines, and the histology facility, University of Lille 2, Professor Défossez and Professor Claude-Alain Maurage for the histological analyses of specimens. We are also grateful to Dr Vincent Prevot for experimental advice and helpful discussions.

Conflict of Interest statement. None declared.

FUNDING

This work was supported by Compagnia di San Paolo (grant number 2008.1224 to P.G.), Turin, Italy; Regione Piemonte Ricerca Sanitaria Finalizzata, Italy; Fondazione CRT ('Progetto Alfieri' and 'Progetto Lagrange'), Turin, Italy; the Institut National de la Santé et de la Recherche Médicale, Inserm, France (grant number U837); Agence Nationale de la Recherche, ANR, France (grant number ANR-2010-JCJC-1404-01 to P.G.); the intramural research program of the NINDS, NIH, Bethesda, MD, USA; the Netherlands Organization for Health Research and Development (ZonMW-VIDI/TOP to J.R.P.), the Human Frontier Science Program (HFSP-CDA to J.R.P.) and the ABC Genomics Center Utrecht and the European Union mdDANeurodev, FP7/2007-2011 (grant number 222999 to J.R.P.).

REFERENCES

1. Wray, S. (2010) From nose to brain: development of gonadotrophin-releasing hormone-1 neurones. *J. Neuroendocrinol.*, **22**, 743–753.
2. Schwanzel-Fukuda, M. and Pfaff, D.W. (1989) Origin of luteinizing hormone-releasing hormone neurons. *Nature*, **338**, 161–164.
3. Wray, S., Grant, P. and Gainer, H. (1989) Evidence that cells expressing luteinizing hormone-releasing hormone mRNA in the mouse are derived from progenitor cells in the olfactory placode. *Proc. Natl Acad. Sci. USA*, **86**, 8132–8136.
4. Pitteloud, N., Durrani, S., Raivio, T. and Sykiotis, G.P. (2010) Complex genetics in idiopathic hypogonadotropic hypogonadism. *Front. Horm. Res.*, **39**, 142–153.
5. Gonzalez-Martinez, D., Hu, Y. and Bouloux, P.M. (2004) Ontogeny of GnRH and olfactory neuronal systems in man: novel insights from the investigation of inherited forms of Kallmann's syndrome. *Front. Neuroendocrinol.*, **25**, 108–130.
6. Caronia, L.M., Martin, C., Welt, C.K., Sykiotis, G.P., Quinton, R., Thambundit, A., Avbelj, M., Dhruvakumar, S., Plummer, L., Hughes, V.A. *et al.* (2011) A genetic basis for functional hypothalamic amenorrhea. *N. Engl. J. Med.*, **364**, 215–225.
7. Wierman, M.E., Kiseljak-Vassiliades, K. and Tobet, S. (2011) Gonadotropin-releasing hormone (GnRH) neuron migration: initiation, maintenance and cessation as critical steps to ensure normal reproductive function. *Front. Neuroendocrinol.*, **32**, 43–52.
8. Cariboni, A., Hickok, J., Rakic, S., Andrews, W., Maggi, R., Tischkau, S. and Parnavelas, J.G. (2007) Neuropilins and their ligands are important in the migration of gonadotropin-releasing hormone neurons. *J. Neurosci.*, **27**, 2387–2395.
9. Cariboni, A., Davidson, K., Rakic, S., Maggi, R., Parnavelas, J.G. and Ruhrberg, C. (2011) Defective gonadotropin-releasing hormone neuron migration in mice lacking SEMA3A signalling through NRP1 and NRP2: implications for the aetiology of hypogonadotropic hypogonadism. *Hum. Mol. Genet.*, **20**, 336–344.
10. Giacobini, P., Messina, A., Morello, F., Ferraris, N., Corso, S., Penachioni, J., Giordano, S., Tamagnone, L. and Fasolo, A. (2008) Semaphorin 4D regulates gonadotropin hormone-releasing hormone-1 neuronal migration through PlexinB1-Met complex. *J. Cell Biol.*, **183**, 555–566.
11. Tran, T.S., Kolodkin, A.L. and Bharadwaj, R. (2007) Semaphorin regulation of cellular morphology. *Annu. Rev. Cell Dev. Biol.*, **23**, 263–292.
12. Zhou, Y., Gunput, R.A. and Pasterkamp, R.J. (2008) Semaphorin signaling: progress made and promises ahead. *Trends Biochem. Sci.*, **33**, 161–170.
13. Comeau, M.R., Johnson, R., DuBose, R.F., Petersen, M., Gearing, P., VandenBos, T., Park, L., Farrah, T., Buller, R.M., Cohen, J.I. *et al.* (1998) A poxvirus-encoded semaphorin induces cytokine production from monocytes and binds to a novel cellular semaphorin receptor, VESPR. *Immunity*, **8**, 473–482.
14. Lange, C., Liehr, T., Goen, M., Gebhart, E., Fleckenstein, B. and Ensser, A. (1998) New eukaryotic semaphorins with close homology to semaphorins of DNA viruses. *Genomics*, **51**, 340–350.
15. Xu, X., Ng, S., Wu, Z.L., Nguyen, D., Homburger, S., Seidel-Dugan, C., Ebens, A. and Luo, Y. (1998) Human semaphorin K1 is glycosylphosphatidylinositol-linked and defines a new subfamily of viral-related semaphorins. *J. Biol. Chem.*, **273**, 22428–22434.
16. Suzuki, K., Okuno, T., Yamamoto, M., Pasterkamp, R.J., Takegahara, N., Takamatsu, H., Kitao, T., Takagi, J., Rennert, P.D., Kolodkin, A.L. *et al.* (2007) Semaphorin 7A initiates T-cell-mediated inflammatory responses through alpha1beta1 integrin. *Nature*, **446**, 680–684.
17. Lazova, R., Gould Rothberg, B.E., Rimm, D. and Scott, G. (2009) The semaphorin 7A receptor Plexin C1 is lost during melanoma metastasis. *Am. J. Dermatopathol.*, **31**, 177–181.
18. Scott, G.A., McClelland, L.A. and Fricke, A.F. (2008) Semaphorin 7a promotes spreading and dendricity in human melanocytes through beta1-integrins. *J. Invest. Dermatol.*, **128**, 151–161.
19. Scott, G.A., McClelland, L.A., Fricke, A.F. and Fender, A. (2009) Plexin C1, a receptor for semaphorin 7a, inactivates cofilin and is a potential tumor suppressor for melanoma progression. *J. Invest. Dermatol.*, **129**, 954–963.
20. Ohsawa, S., Hamada, S., Asou, H., Kuida, K., Uchiyama, Y., Yoshida, H. and Miura, M. (2009) Caspase-9 activation revealed by semaphorin 7A cleavage is independent of apoptosis in the aged olfactory bulb. *J. Neurosci.*, **29**, 11385–11392.
21. Ohsawa, S., Hamada, S., Kuida, K., Yoshida, H., Igaki, T. and Miura, M. (2010) Maturation of the olfactory sensory neurons by Apaf-1/caspase-9-mediated caspase activity. *Proc. Natl Acad. Sci. USA*, **107**, 13366–13371.
22. Pasterkamp, R.J., Peschon, J.J., Spriggs, M.K. and Kolodkin, A.L. (2003) Semaphorin 7A promotes axon outgrowth through integrins and MAPKs. *Nature*, **424**, 398–405.

23. Xu, C. and Fan, C.M. (2007) Allocation of paraventricular and supraoptic neurons requires Sim1 function: a role for a Sim1 downstream gene PlexinC1. *Mol. Endocrinol.*, **21**, 1234–1245.
24. Pasterkamp, R.J., Kolk, S.M., Hellemons, A.J. and Kolodkin, A.L. (2007) Expression patterns of semaphorin7A and plexinC1 during rat neural development suggest roles in axon guidance and neuronal migration. *BMC Dev. Biol.*, **7**, 98–114.
25. Calof, A.L. and Chikaraishi, D.M. (1989) Analysis of neurogenesis in a mammalian neuroepithelium: proliferation and differentiation of an olfactory neuron precursor in vitro. *Neuron*, **3**, 115–127.
26. Miragall, F., Kadmon, G. and Schachner, M. (1989) Expression of L1 and N-CAM cell adhesion molecules during development of the mouse olfactory system. *Dev. Biol.*, **135**, 272–286.
27. Schwanzel-Fukuda, M., Abraham, S., Crossin, K.L., Edelman, G.M. and Pfaff, D.W. (1992) Immunocytochemical demonstration of neural cell adhesion molecule (NCAM) along the migration route of luteinizing hormone-releasing hormone (LHRH) neurons in mice. *J. Comp. Neurol.*, **321**, 1–18.
28. Fueshko, S. and Wray, S. (1994) LHRH cells migrate on peripherin fibers in embryonic olfactory explant cultures: an in vitro model for neurophilic neuronal migration. *Dev. Biol.*, **166**, 331–348.
29. Giacobini, P., Kopin, A.S., Beart, P.M., Mercer, L.D., Fasolo, A. and Wray, S. (2004) Cholecystokinin modulates migration of gonadotropin-releasing hormone-1 neurons. *J. Neurosci.*, **24**, 4737–4748.
30. Giacobini, P. and Wray, S. (2007) Cholecystokinin directly inhibits neuronal activity of primary gonadotropin-releasing hormone cells through cholecystokinin-1 receptor. *Endocrinology*, **148**, 63–71.
31. Kramer, P.R. and Wray, S. (2001) Nasal embryonic LHRH factor (NELF) expression within the CNS and PNS of the rodent. *Gene Expr. Patterns*, **1**, 23–26.
32. Sharifi, N., Reuss, A.E. and Wray, S. (2002) Prenatal LHRH neurons in nasal explant cultures express estrogen receptor beta transcript. *Endocrinology*, **143**, 2503–2507.
33. Radovick, S., Wray, S., Lee, E., Nicols, D.K., Nakayama, Y., Weintraub, B.D., Westphal, H., Cutler, G.B. Jr. and Wondisford, F.E. (1991) Migratory arrest of gonadotropin-releasing hormone neurons in transgenic mice. *Proc. Natl Acad. Sci. USA*, **88**, 3402–3406.
34. Giacobini, P., Giampietro, C., Fioretto, M., Maggi, R., Cariboni, A., Perroteau, I. and Fasolo, A. (2002) Hepatocyte growth factor/scatter factor facilitates migration of GN-11 immortalized LHRH neurons. *Endocrinology*, **143**, 3306–3315.
35. Beltman, J.B., Maree, A.F. and de Boer, R.J. (2009) Analysing immune cell migration. *Nat. Rev. Immunol.*, **9**, 789–798.
36. Cloutier, J.F., Giger, R.J., Koentges, G., Dulac, C., Kolodkin, A.L. and Ginty, D.D. (2002) Neuropilin-2 mediates axonal fasciculation, zonal segregation, but not axonal convergence, of primary accessory olfactory neurons. *Neuron*, **33**, 877–892.
37. Cloutier, J.F., Sahay, A., Chang, E.C., Tessier-Lavigne, M., Dulac, C., Kolodkin, A.L. and Ginty, D.D. (2004) Differential requirements for semaphorin 3F and Slit-1 in axonal targeting, fasciculation, and segregation of olfactory sensory neuron projections. *J. Neurosci.*, **24**, 9087–9096.
38. Giger, R.J., Cloutier, J.F., Sahay, A., Prinjha, R.K., Levengood, D.V., Moore, S.E., Pickering, S., Simmons, D., Rastan, S., Walsh, F.S. *et al.* (2000) Neuropilin-2 is required in vivo for selective axon guidance responses to secreted semaphorins. *Neuron*, **25**, 29–41.
39. Imai, T., Yamazaki, T., Kobayakawa, R., Kobayakawa, K., Abe, T., Suzuki, M. and Sakano, H. (2009) Pre-target axon sorting establishes the neural map topography. *Science*, **325**, 585–590.
40. Schwarting, G.A., Kostek, C., Ahmad, N., Dibble, C., Pays, L. and Puschel, A.W. (2000) Semaphorin 3A is required for guidance of olfactory axons in mice. *J. Neurosci.*, **20**, 7691–7697.
41. Taniguchi, M., Nagao, H., Takahashi, Y.K., Yamaguchi, M., Mitsui, S., Yagi, T., Mori, K. and Shimizu, T. (2003) Distorted odor maps in the olfactory bulb of semaphorin 3A-deficient mice. *J. Neurosci.*, **23**, 1390–1397.
42. Walz, A., Rodriguez, I. and Mombaerts, P. (2002) Aberrant sensory innervation of the olfactory bulb in neuropilin-2 mutant mice. *J. Neurosci.*, **22**, 4025–4035.
43. Kim, S.H., Hu, Y., Cadman, S. and Bouloux, P. (2008) Diversity in fibroblast growth factor receptor 1 regulation: learning from the investigation of Kallmann syndrome. *J. Neuroendocrinol.*, **20**, 141–163.
44. Herbison, A.E., Porteous, R., Pape, J.R., Mora, J.M. and Hurst, P.R. (2008) Gonadotropin-releasing hormone neuron requirements for puberty, ovulation, and fertility. *Endocrinology*, **149**, 597–604.
45. Gamble, J.A., Karunadasa, D.K., Pape, J.R., Skynner, M.J., Todman, M.G., Bicknell, R.J., Allen, J.P. and Herbison, A.E. (2005) Disruption of ephrin signaling associates with disordered axophilic migration of the gonadotropin-releasing hormone neurons. *J. Neurosci.*, **25**, 3142–3150.
46. Schwarting, G.A., Raitcheva, D., Bless, E.P., Ackerman, S.L. and Tobet, S. (2004) Netrin 1-mediated chemoattraction regulates the migratory pathway of LHRH neurons. *Eur. J. Neurosci.*, **19**, 11–20.
47. Pitteloud, N., Zhang, C., Pignatelli, D., Li, J.D., Raivio, T., Cole, L.W., Plummer, L., Jacobson-Dickman, E.E., Mellon, P.L., Zhou, Q.Y. *et al.* (2007) Loss-of-function mutation in the prokineticin 2 gene causes Kallmann syndrome and normosmic idiopathic hypogonadotropic hypogonadism. *Proc. Natl Acad. Sci. USA*, **104**, 17447–17452.
48. Perala, N.M., Immonen, T. and Sariola, H. (2005) The expression of plexins during mouse embryogenesis. *Gene Expr. Patterns*, **5**, 355–362.
49. Casazza, A., Fazzari, P. and Tamagnone, L. (2007) Semaphorin signals in cell adhesion and cell migration: functional role and molecular mechanisms. *Adv. Exp. Med. Biol.*, **600**, 90–108.
50. Chung, W.C., Moyle, S.S. and Tsai, P.S. (2008) Fibroblast growth factor 8 signaling through fibroblast growth factor receptor 1 is required for the emergence of gonadotropin-releasing hormone neurons. *Endocrinology*, **149**, 4997–5003.
51. Seminara, S.B. and Crowley, W.F. Jr. (2008) Kisspeptin and GPR54: discovery of a novel pathway in reproduction. *J. Neuroendocrinol.*, **20**, 727–731.
52. Xu, N., Kim, H.G., Bhagavath, B., Cho, S.G., Lee, J.H., Ha, K., Meliciani, I., Wenzel, W., Podolsky, R.H., Chorich, L.P. *et al.* (2011) Nasal embryonic LHRH factor (NELF) mutations in patients with normosmic hypogonadotropic hypogonadism and Kallmann syndrome. *Fertil. Steril.*, **95**, 1613–1620e7.
53. Levi, G., Mantero, S., Barbieri, O., Cantatore, D., Paleari, L., Beverdam, A., Genova, F., Robert, B. and Merlo, G.R. (2006) Msx1 and Dlx5 act independently in development of craniofacial skeleton, but converge on the regulation of Bmp signaling in palate formation. *Mech. Dev.*, **123**, 3–16.
54. Kramer, P.R. and Wray, S. (2000) Novel gene expressed in nasal region influences outgrowth of olfactory axons and migration of luteinizing hormone-releasing hormone (LHRH) neurons. *Genes Dev.*, **14**, 1824–1834.
55. Serini, G., Valdembri, D., Zanivan, S., Morterra, G., Burkhardt, C., Caccavari, F., Zammataro, L., Primo, L., Tamagnone, L., Logan, M. *et al.* (2003) Class 3 semaphorins control vascular morphogenesis by inhibiting integrin function. *Nature*, **424**, 391–397.
56. Knöll, B., Weinl, C., Nordheim, A. and Bonhoeffer, F. (2007) Stripe assay to examine axonal guidance and cell migration. *Nat. Protoc.*, **2**, 1216–1224.